Astron. Astrophys. 316, 304–312 (1996)

ASTRONOMY
AND
ASTROPHYSICS

Latitudinal dependence of the radial IMF component - interplanetary imprint

S.T. Suess[1], **E.J. Smith**[2], **J. Phillips**[3], **B.E. Goldstein**[2], **and S. Nerney**[4]

[1] NASA Marshall Space Flight Center, MS ES82, Huntsville, AL 35812, USA
[2] MS 169-506, Jet Propulsion Laboratory, 4800 Oak Grove Dr., Pasadena, CA 91109-8099, USA
[3] MS D438, Los Alamos National Laboratory, Los Alamos, NM 87545, USA
[4] 1570 Granville Pike, Ohio University, Lancaster, OH 43130, USA

Received 15 February 1996 / Accepted 14 June 1996

Abstract. Ulysses measurements have confirmed that there is no significant gradient with respect to heliomagnetic latitude in the radial component, B_r, of the interplanetary magnetic field. There are two processes responsible for this observation. In the corona, the plasma β is $\ll 1$, except directly above streamers, so both longitudinal and latitudinal (meridional) gradients in field strength will relax, due to the transverse magnetic pressure gradient force, as the solar wind carries magnetic flux away from the Sun. This happens so quickly that the field is essentially uniform by 5 $R_\odot$. Beyond 10 $R_\odot$, $\beta > 1$ and it is possible for a meridional thermal pressure gradient to redistribute magnetic flux - an effect apparently absent in Ulysses and earlier ICE and IMP data. We discuss this second effect here, showing that its absence is mainly due to the perpendicular part of the anisotropic thermal pressure gradient in the interplanetary medium being too small to drive significant meridional transport between the Sun and ~ 4 AU. This is done using a linear analytic estimate of meridional transport. The first effect was discussed in an earlier paper.

Key words: Sun; corona; solar wind; magnetic field

1. Introduction

Ulysses in 1993-1995 (Smith and Balogh, 1995; Balogh et al. 1995) and ICE and IMP-8 in 1984-1988 (Burton et al. 1995) observed no significant gradient in heliomagnetic latitude in the radial component of the interplanetary magnetic field (IMF) at heliocentric distances of 1-4 AU. These observations were made near solar minimum when the Sun's magnetic field is nearly an axially aligned dipole. Fig. 1 shows the results from IMP-8 and ICE scaled to 1 AU and plotted against magnetic latitude. The data are five degree latitude bin averages. The solid line is a simple equatorial current sheet model of the IMF which, outside a few tens of solar radii, gives a uniform field in the two hemispheres (Wolfson, 1985) and is a good approximation to the radial component, B_r, of the IMF at those distances. The apparent appearance of a small gradient in the radial component of the field near the equator in Fig. 1 is probably all due to small errors in magnetic sector identification so that the true gradient is completely negligible. No gradient at all was seen by Ulysses in 1993-1995 up to heliographic latitudes of $\pm 80.22^o$.

It was shown in an earlier paper (Suess and Smith, 1996) that the field strength at the top of the corona, $\sim$ 10 $R_\odot$, has no significant gradient in latitude or longitude outside of the heliospheric plasma sheet (HPS) which exists above streamers (Gosling et al. 1981).

This is a consequence of the plasma β, the ratio of thermal pressure to magnetic pressure, being $\ll 1$ inside 10 $R_\odot$ except in the HPS. Beyond this distance, $\beta > 1$, at least to well beyond the orbit of Jupiter, except in some transients. Therefore, between the top of the corona and several AU, meridional gradients in the thermal pressure may redistribute magnetic flux in latitude. A linear analytic model is used here to analyze the Ulysses data for the effect of meridional gradients in the density, temperature, and flow speed on the meridional distribution of magnetic flux.

It has already been suggested by Suess et al. (1977) that the thermal pressure gradient may indeed have a measurable effect. Suess et al. utilized a semi-analytic MHD model of coronal hole flow to simulate the northern polar coronal hole observed from Skylab in 1973 and described by Munro and Jackson (1977). Their model, when carried to 1 AU, implied that meridional redistribution of mass and magnetic flux between the high corona and 1 AU might be a significant process. Results shown in Fig. 2 from the Suess et al. model illustrate the variation of the radial magnetic field with colatitude at 2.0 $R_\odot$, 5.0 $R_\odot$, and 1 AU. Panel (a) shows what is actually the boundary condition at 2 $R_\odot$, a smooth, dipole field. To understand panels (b) and (c), a little more must be said about the model. Briefly, it is polytropic with an index $\gamma = 1.05$ and is therefore nearly isothermal in radius, although the temperature varies strongly with latitude. The plasma β is less than unity in the corona, but is larger than

Send offprint requests to: S.T. Suess

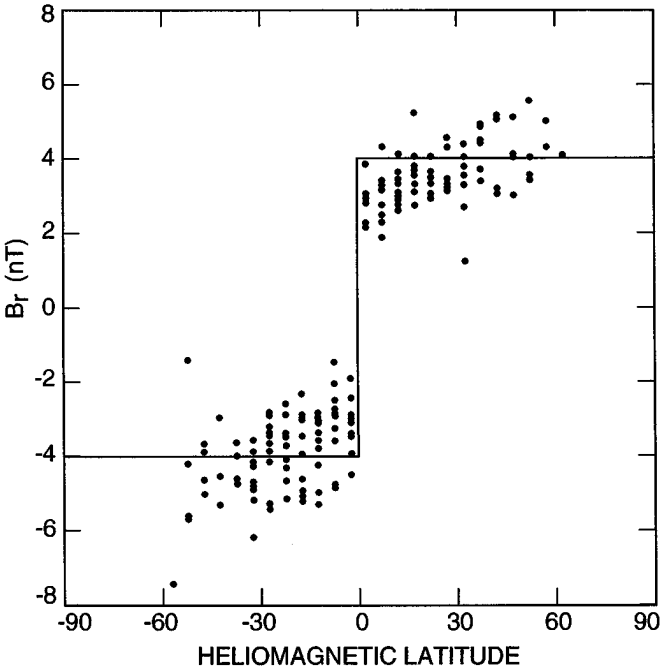

Fig. 1. Radial magnetic field values in five degree latitude bins, scaled to 1 AU, from ICE and IMP-8 during 1984-1988, bracketing solar minimum, and Ulysses during 1993-1994, also at the time of solar minimum (Burton et al. 1995). The solid line which is discontinuous at the equator is from a simple current sheet model (Wolfson, 1985) at a heliocentric distance of more than ca. 50 $R_\odot$.

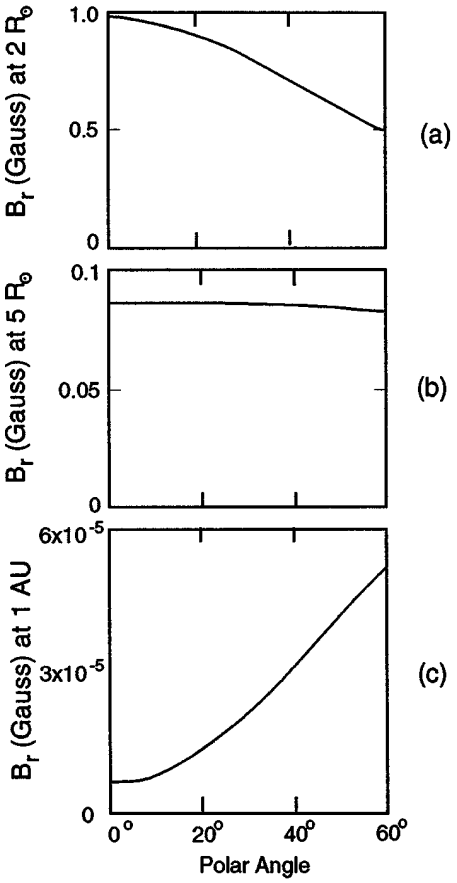

Fig. 2a–c. The radial magnetic field variation between $\theta = 0^o$ (north pole) and $\theta = 60^o$, at **a** 2 $R_\odot$, **b** 5 $R_\odot$, **c** 1 AU, from the MHD model of the 1973 polar coronal hole of Suess et al. (1977).

unity beyond $5-10\,R_\odot$. The effects both of the relaxation, with increasing radius, of meridional gradients in magnetic pressure in the corona (Suess and Smith, 1996) and of the interplanetary thermal pressure gradient can be seen in this figure. Panel (b) shows that the field is almost independent of colatitude at 5 $R_\odot$ due to the relaxation of the meridional magnetic pressure gradient in the low β corona. Panel (c) shows that a large variation in B_r is reintroduced between 5 $R_\odot$ and 1 AU by the interplanetary meridional thermal pressure gradient.

While Suess et al. successfully simulated the observed coronal hole properties, the IMP and ICE results shown in Fig. 1 demonstrate that the conditions at 1 AU predicted by their model did not exist at the time those observations were made, or at the time the more recent Ulysses observations were made (Smith and Balogh, 1995; Balogh, et al. 1995). The failure of the model to reproduce the Ulysses, ICE, and IMP observations is due both to the model pressure and the meridional pressure gradient in the interplanetary medium being too large. The large pressure is a consequence of using $\gamma = 1.05$ so that the temperature at 1 AU is between 0.5×10^6 and 1.0×10^6 K - larger than observed. The large pressure gradient is due to the large temperature variation across the model coronal hole. When combined with the predicted density, this leads to a large meridional pressure gradient that redistributes mass and momentum flux. In principle, that model could be utilized again to analyze Ulysses data and understand the absence of interplanetary meridional transport. However, the problem is physically and mathematically somewhat simpler than modeling coronal flow where radial gradients in the flow speed are large. Therefore, we instead describe a simpler, fully analytic analysis of the data.

The result we find is suprising. Using the simplest assumptions that the pressure is isotropic and that the meridional pressure gradient acts uniformly all the way from 10 $R_\odot$ to 4 AU leads to a contradiction. A substantial meridional flow and redistribution of magnetic flux is predicted at 4 AU, contrary to observation. Apparently the main reason for this is that the pressure in the solar wind is anisotropic and, together with a consideration of how the effective pressure may vary with heliocentric distance, we find that Ulysses and other data for the pressure anisotropy are entirely consistent with only a small meridional redistribution of magnetic flux at 4 AU. This is, therefore, an example of a breakdown in the simplest form of the isotropic fluid equations in application to the large scale dynamics of the solar wind.

2. Analytic estimate of meridional transport due to a meridional thermal pressure gradient

We consider the solar wind to be described by the ideal MHD equations for a single fluid and we apply these to analyzing the

extent a merdional thermal pressure gradient can redistribute magnetic (and mass) flux in the interplanetary medium between 10 $R_\odot$ and 1-4 AU, a region in which $\beta > 1$. Assumptions can be made for this specific problem which make the analytic treatment tractable and simple. Including those stated above, these are:

(1) The flow is nearly (but not exactly) radial.
(2) The radial flow speed is independent of radius.
(3) Magnetohydrodynamic effects are negligible.
(4) Gravity is negligible.
(5) The flow is axisymmetric.

Assumption (1) is valid beyond 5 $R_\odot$, except during large transients (which are not under consideration here). (2) is sufficiently well satisfied to permit an estimate of whether meridional mass and magnetic flux transport is a large effect at 1-4 AU. It is not necessarily sufficiently accurate to permit a quantitative calculation of meridional transport. (3) has been evaluated elsewhere to show that MHD effects are smaller than, and hence can be treated separately from, thermal pressure gradient effects (Suess and Nerney, 1975a,b). (4) follows simply by knowing the solar wind flow is supersonic and from comparison of the kinetic energy with the gravitational potential energy. With regard to (5), the Ulysses fast latitude scan in 1994-1995 was just prior to solar minimum, when the Sun's magnetic field might reasonably be approximated as an axisymmetric dipole. At other times, the results we find here would only be applicable, at best, to properties averaged over a solar rotation period. This may be a weak assumption when there exist large corotating interaction regions, as shown by Pizzo and Goldstein (1987).

Under the above assumptions, the solution to meridional transport can be estimated using a "quasi-radial flow" approximation (Suess and Nerney, 1975a). Consider **B**, **v**, n, and T to be written as

$$\mathbf{B} = \mathbf{B}_1 + \mathbf{B}_2 + ... \tag{1a}$$

$$\mathbf{v} = \mathbf{v}_1 + \mathbf{v}_2 + ... \tag{1b}$$

$$n = n_1 + n_2 + ... \tag{1c}$$

$$T = T_1 + T_2 + ... \tag{1d}$$

where $\mathbf{v}_1 = \hat{e}_r v_{1r}$ and it is assumed that $| \mathbf{B}_2 | \ll | \mathbf{B}_1 |$, $| \mathbf{v}_2 | \ll | \mathbf{v}_1 |$, etc. Terms of O[1], those with subscript '1', are collected together to produce Eqs. (2) and the O[1] solution. Terms of O[$\mathbf{B}_2, \mathbf{v}_2, n_2, T_2$] are collected to find the next "higher order" equations. The derivation shown here is fully and completely described below, but does not include some "back pressure" terms which would limit flux redistribution in latitude if it becomes an O[1] effect. Such might be the case in the outer heliosphere and will be the subject of a more comprehensive analysis elsewhere. A general discussion of perturbation expansions of differential equations is given, for example, by Cole (1968).

The "lowest order" equations describing the solar wind in the present approximation are then $v_{1r} \equiv \mathrm{V}_r(\theta)$ and

$$\frac{1}{r^2}\frac{d}{dr}(r^2 n_1(r,\theta)\mathrm{V}_r(\theta)) = 0 \tag{2a}$$

$$\frac{1}{r^2}\frac{d}{dr}(r^2 B_{1r}(r)) = 0 \tag{2b}$$

or

$$n_1(r,\theta) = n_E(\theta)\left(\frac{r_E}{r}\right)^2 \tag{2c}$$

$$B_{1r}(r) = B_{or}\left(\frac{r_o}{r}\right)^2 \tag{2d}$$

where B_{or} is the value at the top of the corona, $r_o = 10\ R_\odot$, beyond which distance β is greater than unity, and the density at 1 AU, $n_E(\theta)$, is from Ulysses observations scaled to 1 AU$\equiv r_E$. Because of the results from Suess and Smith (1996), it can be taken that $B_{or} \neq$ a function of θ. The parameters defining $n_E(\theta)$ and the temperature will be determined empirically, using Ulysses data. There is no momentum equation to this order because $\mathrm{V}_r(\theta)$ is independent of radius. There is a meridional pressure gradient, $\partial p_1/\partial\theta$, but its dynamic effect in producing a meridional flow is shown below to be scaled by M^{-2}, where M is the Mach number. Therefore, the meridional momentum equation is of the next higher order, and is used to determine the the absolute magnitude of the higher order effects. The resulting meridional flow in turn modifies the mass and magnetic flux distribution.

Four equations will be involved in computing the meridional transport - the meridional component of the momentum equation, the continuity equation, the solenoidal condition, and the induction equation. Eqs. (2) described the lowest order solution. In the next order, the linearized meridional momentum equation is given by:

$$m_p n_1(r,\theta)\frac{\mathrm{V}_r(\theta)}{r}\frac{\partial}{\partial r}(r v_{2\theta}(r,\theta)) = -\frac{1}{r}\frac{\partial p_1}{\partial\theta} \tag{3}$$

where the formula has been written in such a way as to emphasize that the lowest order flow field (subscript '1') provides the forcing function to the next higher order (subscript '2') response of the solar wind. This ordering only works if the solution ($T_2, \mathbf{B}_2, \mathbf{v}_2, n_2$) remains small relative to the lowest order solution. The rest of the equations in this order are

$$v_{2\theta}(r,\theta)B_{1r}(r) - \mathrm{V}_r(\theta)B_{2\theta}(r,\theta) = 0 \tag{4a}$$

$$\frac{1}{r^2}\frac{\partial}{\partial r}(r^2 B_{2r}(r,\theta)) + \frac{1}{r\sin\theta}\frac{\partial}{\partial\theta}(B_{2\theta}(r,\theta)\sin\theta) = 0 \tag{4b}$$

$$\frac{1}{r^2}\frac{\partial}{\partial r}(r^2 n_2(r,\theta)\mathrm{V}_r(\theta)) + \frac{1}{r\sin\theta}\frac{\partial}{\partial\theta}(n_1(r,\theta)v_{2\theta}(r,\theta)\sin\theta) = 0 \tag{4c}$$

Eq. (3) can be seen to be a valid linearization in the supersonic solar wind if it is written in dimensionless form by scaling the velocity, density, and the temperature with their values (v_{1r}, n_E, T_E) at 1 AU for an arbitrary value of $\theta = \theta_E$. Then, with primes denoting dimensionless variables

$$\frac{\partial(r' v'_{2\theta}(r',\theta))}{\partial r'} = -\frac{1}{M_E^2}\frac{1}{\rho'\mathrm{V}'_r(\theta)}\frac{\partial p'_1(r',\theta)}{\partial\theta} \tag{5}$$

In words, the O[1] merdional gradient in p_1 leads to an O[$1/M_E^2$] meridional flow, $v'_{2\theta}(r',\theta)$, where M_E^2 is the square of the Mach number at 1 AU, at the polar angle $\theta = \theta_E$. Since $M_E^2 >> 1$ in the supersonic solar wind, $[v'_{2\theta}(r',\theta)] << [\mathrm{V}'_r(\theta)]$. There are, of course, other terms in the full meridional momentum equation. These include a term of O[$v^2_{2\theta}(r,\theta)$], which is of O[$1/M_E^4$] and hence ignorable. They also include a term of order $p'_2(r',\theta)$ which would have to be as large as M_E^2 to be important. This is the back pressure referred to earlier which limits the redistribution of flux when it becomes large. Other terms are ignored under the assumptions listed at the beginning of Sect. 2. With regard to the rest of the equations which determine $v_{2\theta}(r,\theta)$, (4a) is the azimuthal component of the induction equation, and (4b) and (4c) are the solenoidal condition and the continuity equation, respectively, to this order.

The solution procedure is the following. Empirical functions for $\mathrm{V}_r(\theta)$, $p_1(r,\theta)$, $n_1(r,\theta)$, and $T_1(r,\theta)$ are used in (3) to compute $v_{2\theta}(r,\theta)$. This is used in (4a) to find $B_{2\theta}(r,\theta)$. Eqs. (4b) and (4c) are then solved for $n_2(r,\theta)$ and $B_{2r}(r,\theta)$. The latter is the desired dependent variable since it describes the redistribution of magnetic flux by the meridional pressure gradient. The overall result is given by

$$B_r(r,\theta) = B_{1r}(r) + B_{2r}(r,\theta) \tag{6}$$

It remains to specify the empirically determined analytic forms of $p_1(r,\theta)$, $n_1(r,\theta)$, $\mathrm{V}_r(\theta)$, and $T_1(r,\theta)$.

3. Application of Ulysses fast latitude scan observations to the evaluation of meridional transport

We first turn to the empirical determination of n_1 and T_1, and we also combine the plasma data with Ulysses magnetometer data to show that $\beta > 1$, justifying assumption (3) above. The Ulysses solar wind plasma instrument measures the ion and electron plasma distributions, from which the temperature, density, and pressure can be determined (Phillips et al. 1995). Ion and electron temperature radial gradients are not well determined, but other empirical determinations give the non-adiabatic dependence of these temperatures on radius as approximately $r^{-0.7}$ (Phillips et al., 1995). Here, we will adopt this dependence but will later discuss the effect of other choices such as the $r^{-0.5}$ dependence found by Richardson et al. (1995) in the IMP 8 and Voyager 2 data. Any empirical radial dependence is easily utilized in the analytic evaluation.

The total pressure of the plasma is then given by $p = k(n_pT_p + n_\alpha T_\alpha + n_eT_e)$, where (n_p, n_α, n_e) and (T_p, T_α, T_e) are the number densities and temperatures of protons, alpha particles, and electrons, respectively. n_e is, occasionally, not accurately measured and therefore is replaced by $(n_p + 2n_\alpha) = n_e$. The proton and alpha particle temperatures are the one dimensional temperatures in the energy direction over full field of view. This is the most accurate temperature available from the Ulysses SWOOPS data.

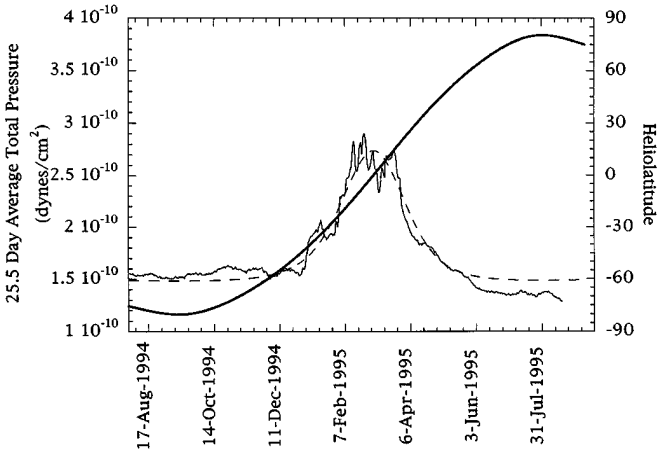

Fig. 3. 25.5 day running averages of the thermal pressure at Ulysses, scaled to 1 AU as described in the text. Also shown are the heliographic latitude of Ulysses and the curve fit to the pressure data that is described in the text.

Using the above radial variation, the observed total thermal pressure can be scaled to 1 AU. This quantity is subject to large fluctuations due to transient disturbances. Therefore, for the purposes of studying global scale meridional redistribution of mass and magnetic flux, running averages over 25.5 days (one solar rotation) are used. Averages are computed as the average of products. The result is shown in Fig. 3, along with the heliographic latitude of Ulysses, for the interval of the Ulysses fast latitude scan between 1 August 1994 and 1 September 1995.

The observations shown in Fig. 3 were made over a brief one year interval so that global solar conditions are relatively constant. Plasma data from this interval have been reported in more detail by Phillips et al. (1995). The normalized pressure can be seen to be of O[$1.5 - 2$] $\times 10^{-10}$ dynes/cm^2 over most of the interval, being approximately constant from 80.22^o S to 50^o S and again from 50^o N to 80.22^o N. The pressure probably continues at about the same value all the way to the North and South poles because at the higher latitudes Ulysses was fully immersed in the polar high speed streams. However, between 50^o S and 50^o N the pressure increases by about 50%, maximizing at the equator. Therefore, there is a pressure maximum at the equator with a relatively narrow half-width that is approximately symmetric across the equator. A curve has been fit in Fig. 3 (dashed curve) to the pressure variation. Using a scaling in radius of density $\propto r^{-2}$ and temperature $\propto r^{-0.7}$ (Phillips et al., 1995) to define the radial variation of the pressure, the equation for the curve fit is given by

$$p_1(r,\theta) = p_E \left(1 + \epsilon e^{-\alpha \cos^2\theta}\right) \left(\frac{r_E}{r}\right)^{2.7} \tag{7}$$

The parameters for the fit shown in Fig. 3 are $p_E = 1.44 \times 10^{-10}$ dyne-cm^2, $\alpha = 3.5$, and $\epsilon = 0.9$. This will serve for examining whether meridional pressure gradients might cause significant mass and magnetic flux redistribution.

Before applying (7), we first consider the plasma β, found by combining the pressure shown in Fig. 3 with the total magnetic

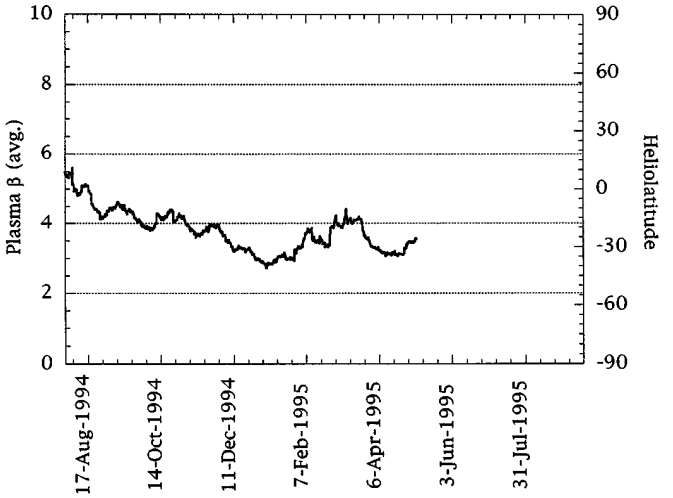

Fig. 4. 25.5 day running averages of the plasma β at Ulysses during the fast latitude scan, scaled to 1 AU. The radial magnetic field is scaled as r^{-2} and the transverse field as r^{-1}. The temperature and density are scaled as described in the text.

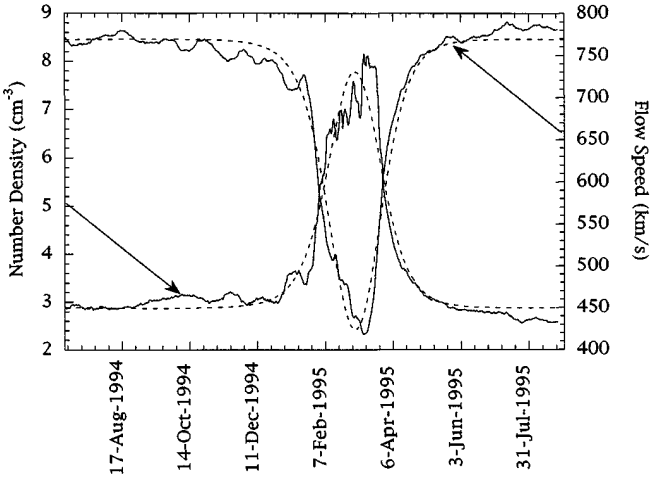

Fig. 5. Density and radial flow speed versus time for Ulysses during the fast latitude scan. The density is scaled to 1 AU as r^{-2}. 25.5 day running averages of the data has been used in both the density and velocity plots. Curve fits to the data are superimposed, with the parameters given in the text.

field strength at Ulysses, scaled to 1 AU, with a running average over 25.5 days. These results are shown in Fig. 4, for the interval covered in Fig. 3. Over the entire interval $\beta \geq 3$ and it can therefore reasonably be asserted that MHD effects are relatively small, as required by assumption (3).

Now, carrying out the integration of Eqs. (3) and (4) described in Sect. 2 results in the following solution:

$$v_{2\theta}(r,\theta) = -\frac{\alpha\epsilon p_E}{0.3 m_p n_E(\theta) \mathrm{V}_r(\theta)} \sin 2\theta e^{-\alpha\cos^2\theta} \times \left(\frac{r_E^{0.7}}{r}\right)(r^{0.3} - r_o^{0.3}) \quad (8a)$$

$$B_{2\theta}(r,\theta) = -\frac{\alpha\epsilon p_E B_{ro}(r_o/r)^2}{0.3 m_p n_E(\theta) \mathrm{V}_r^2(\theta)} \sin 2\theta e^{-\alpha\cos^2\theta} \times \left(\frac{r_E^{0.7}}{r}\right)(r^{0.3} - r_o^{0.3}) \quad (8b)$$

$$B_{2r}(r,\theta) = \frac{2\alpha\epsilon p_E B_o r_o^2 r_E^{0.7}}{0.3 n_E(\theta) m_p \mathrm{V}_r^2(\theta) r^2} \times \left[-\frac{1}{0.7}\left(r^{-0.7} - r_o^{-0.7}\right) + r_o^{0.3}\left(r^{-1} - r_o^{-1}\right)\right] \times \left[2\cos^2\theta - \sin^2\theta - 2\alpha\sin^2\theta\cos^2\theta - \left(\frac{1}{n_E}\frac{dn_E}{d\theta} + \frac{2}{\mathrm{V}_r}\frac{d\mathrm{V}_r}{d\theta}\right)\cos\theta\right] e^{-\alpha\cos^2\theta} \quad (8c)$$

At this point, we can now answer the posed question; how much does the observed meridional thermal pressure gradient redistribute magnetic flux between 10 $R_\odot$ and 1-4 AU?

To do this, it is easier to write (8c) in terms of the ratio between B_{2r} and B_{1r}, to give

$$\frac{B_{2r}(r,\theta)}{B_{1r}(r)} = \frac{2\alpha\epsilon p_E (r_E/r_o)^{0.7}}{0.3 n_E(\theta) m_p \mathrm{V}_r(\theta)^2} \left[\left(\frac{r_o}{r} - 1\right) - \frac{1}{0.7}\left(\left(\frac{r_o}{r}\right)^{0.7} - 1\right)\right] \times \left[2\cos^2\theta - \sin^2\theta - 2\alpha\sin^2\theta\cos^2\theta - \left(\frac{1}{n_E}\frac{dn_E}{d\theta} + \frac{2}{\mathrm{V}_r}\frac{d\mathrm{V}_r}{d\theta}\right)\cos\theta\right] e^{-\alpha\cos^2\theta} \quad (9)$$

This result depends on the individual velocity and density meridional gradients, in addition to the overall meridional pressure gradient. The density and velocity variations are shown in Fig. 5 in the same manner as for the pressure in Fig. 3.

That is, 25.5 day running averages are made. The density is scaled to 1 AU as r^{-2} and the velocity is assumed independent of radius. Then the two sets of data are fit by the same functional form used for the pressure:

$$\mathrm{V}_r(\theta) \equiv v_o\left(1 + \epsilon_v e^{-\alpha_v\cos^2\theta}\right) \quad (10a)$$

$$n_E(r,\theta) \equiv n_{oE}\left(1 + \epsilon_N e^{-\alpha_N\cos^2\theta}\right) \quad (10b)$$

The curve fits in Fig. 5 are for $v_o = 771$ km/s, $\epsilon_v = -0.45$, $\alpha_v = 5.5$ and $n_{oE} = 2.85$ cm^{-3}, $\epsilon_n = 1.73$, $\alpha_n = 5.5$. These are substituted into (9), which can then be abbreviated by

$$\frac{B_{2r}(r,\theta)}{B_{1r}(r)} = C f_1(r) f_2(\theta) \quad (11)$$

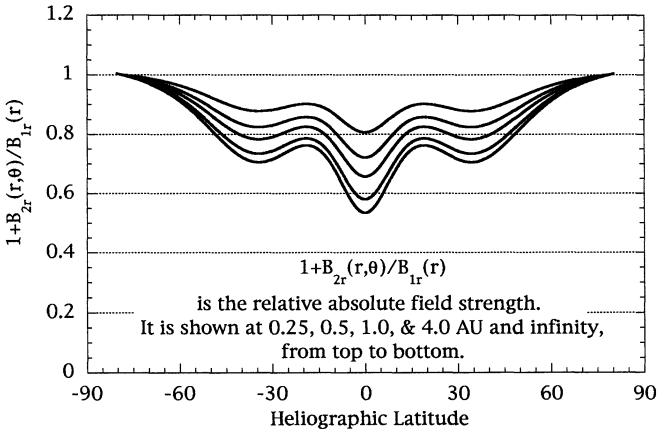

Fig. 6. The relative variation of the modeled magnetic field strength versus heliographic latitude at 0.25, 0.5, 1.0, and 4.0 AU and at $r \rightarrow \infty$ (from top to bottom). This is from Eq. (11).

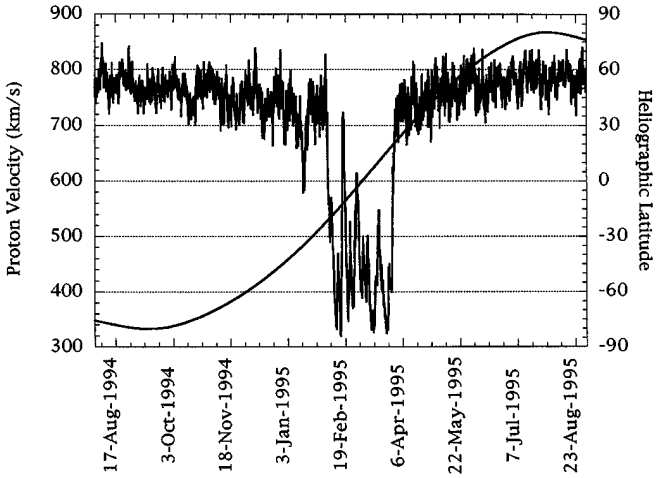

Fig. 7. One hour averages of the radial flow speed over the interval of the Ulysses fast latitude scan. The slot around the heliographic equator, which lies over the solar streamer belt, is seen here to have a series of high speed streams.

where $C = 0.92$, to give

$$\frac{B_{2r}(r,\theta)}{B_{1r}(r)}\,|_{1AU} = 0.28 f_2(\theta) \tag{12a}$$

$$\frac{B_{2r}(r,\theta)}{B_{1r}(r)}\,|_{r\rightarrow\infty} = 0.39 f_2(\theta) \tag{12b}$$

The result suggested by Eq. (12) is significant. It is that flux redistribution due to the pressure, density, and velocity meridional gradients illustrated in Figs. 3 and 5 is not negligible. Fig. 6 shows a plot of Eq. (9) (or, equivalently, Eq. (11)), for the given parameters, for the relative variation of the absolute field strength at 0.25, 0.5, 1.0, and 4.0 AU and infinitely far from the Sun. A broad, deep deficit in radial magnetic flux is predicted around the equator, with a magnitude of approximately 25% far from the Sun. Not only is B_{2r}/B_{1r} not negligible, but also $v_{2\theta}$ given by (8a), using the above parameters, is not negligible. The maximum value of $v_{2\theta}$, which occurs about 35^o away from the equator, is 17 km/s at 1 AU and 8 km/s at 4 AU. A meridional flow this large would probably be observable by the solar wind plasma instrument on Ulysses.

We now must ask why the predicted result based on simple hydrodynamics differs from the observations. With regard to the linearization, $M_E^2 >> 1$ and $v_{2\theta} << v_{1r}$ throughout the solution domain, so the calculation is a mathematically valid estimate of the effect of the meridional pressure gradient.

There are important reasons why the simple hydrodynamic result may not be applicable to the solar wind. One reason has to do with assumption (5), which was that the flow is axisymmetric, or that stream interaction effects are negligible. Fig. 7 is a plot of the 1-hour solar wind speed measurements made at Ulysses throughout the fast latitude scan. A wide range of flow speeds is seen to occur in the region around the heliographic equator. This is precisely the same location as the pressure bump shown in Fig. 3. There are therefore corotating and/or transient high speed streams throughout the latitude range of the streamer belt. The equatorial measurements were made at around 1.4 AU, where the streams are expected to have undergone some dynamic interaction and steepening. This is probably the source of some of the temperature (and hence pressure) increase in this range of heliographic latitudes. It was explicitly assumed above that the pressure bump originated at the Sun and exists continuously out into the solar wind. If, however, the pressure bump is partly due to stream interaction then the bump will not develop until a distance that is a large fraction of an astronomical unit. This process and the associated meridional transport has already been investigated in some detail by Pizzo and Goldstein (1987) in a numerical model of stream interaction. They found what has been shown again here analytically - that a narrow, steep-sided bump in the structure of the equatorial solar wind is able to cause a strong meridional transport of magnetic flux. Their calculations began at 1 AU for the specific reason that stream interaction is relatively negligible inside that distance. The Ulysses measurements during the fast latitude scan were made between 1.34 AU at perihelion, 2.29 AU at -80.22 degrees heliolatitude, and 2.02 AU at +80.22 degrees. It can be expected that stream interaction is therefore somewhat more important than at 1 AU. In terms of the present model calculation, it means a revision in the assumptions and the analysis would have to be made to take into account that the pressure bump had a different (smaller) relative magnitude closer to the Sun.

To simulate the effect of an equatorial pressure bump which increases with heliocentric distance, the radial dependence of the temperature which enters into $f_1(r)$ in Eq. (11) can be changed. This can be used to examine the effect of heating due to stream interaction. In the present case, $T \sim 2 \times 10^6$ K at 10 $R_\odot$. The problem with this is that this temperature is probably higher than exists at that height in the corona because the extrapolation was based on an *in situ* temperature that included some heating due to stream interaction. Therefore, the effect of the meridional pressure gradient near the Sun is overemphasized. The pressure given by (7) therefore overemphasizes the flux

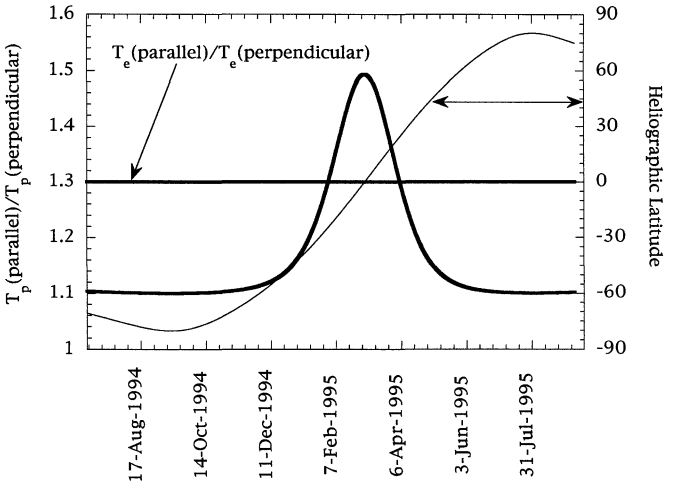

Fig. 8. The assumed proton temperature anisotropy at 1-4 AU as a function of latitude during the Ulysses fast latitude scan. The anisotropy reaches 1.5 at the equator and falls to 1.1 at the poles. The same variation is assumed to apply to alpha particles. The electron anisotropy at the time, also shown, is taken to be 1.3 at all latitudes. These assumed values are used to compute the effective perpendicular pressure from the observed pressure shown in Fig. 3.

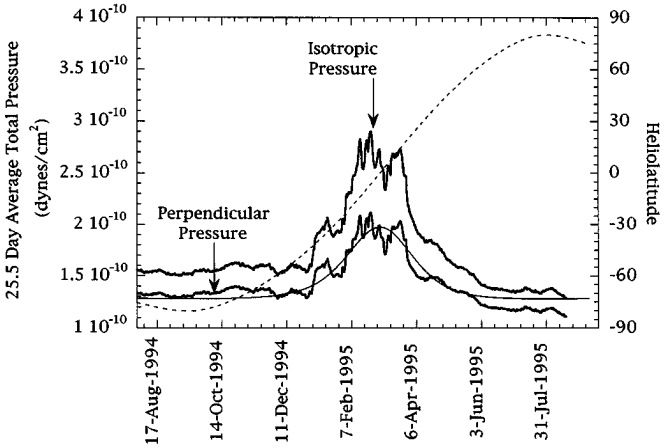

Fig. 9. The 25.5 day running average perpendicular proton temperature during the Ulysses fast latitude scan using the assumed anisotropy shown in Fig. 8. The thin line is a curve fit to the data using Eq. (2), with the parameters $\alpha = 3.33$, $\epsilon = .58$, and $p_E = 1.25 \times 10^{-10}$ dynes/cm^2. The isotropic pressure from Fig. 3 is also shown for reference.

redistribution effect near the Sun. Simply changing the exponent for the temperature dependence can partially simulate this effect. In the extreme case, the temperature could be assumed independent of radius. In this case it turns out that in Eq. (11), $f_1(r) \propto \ln(r)$! This means that while there is a relatively smaller flux redistribution inside 4 AU, there may be a large effect in the outer heliosphere. An alternative assumption might be to take half the pressure bump to be due to stream interaction. The result in this case is that the effect in Eq. (11) is simply halved as well.

Therefore, stream interaction can reduce the flux redistribution, but does not seem to be able to reduce it to the observed levels for strong corotating interaction region heating. Furthermore, it is not obvious that corotating interaction regions are producing much heating in CIRs during the the Ulysses fast latitude scan. The streams shown in Fig. 7 are small in comparison to the model streams invoked by Pizzo and Goldstein (1987) to illustrate CIR effects. Conversely, streamers are known to produce high temperatures and densities in the HPS, as shown by empirical results and streamer models (J. Phillips, priv. comm., Suess et al., 1996).

What apparently has a far more important effect on the pressure gradient driving meridional flux redistribution is the pressure anisotropy. As noted above, the proton and alpha particle temperatures used in computing the pressure shown in Fig. 3 are the one dimensional temperatures in the energy direction (approximately the radial direction) over the full field of view. However, it is the perpendicular temperature in the meridional direction that gives the effective meridional pressure gradient. The electron, proton, and alpha particle anisotropies are measured by SWOOPS on Ulysses and, although the data have not yet been fully reduced, preliminary results indicate that the electron anisotropy is approximately 1.3 everywhere, while the proton anisotropy is approximately 1.1 in the high speed flow and 1.5 in the low speed flow (Goldstein et al., 1995; Goldstein, Neugebauer, and Smith, 1995; Goldstein et al., 1996).

An extensive previous study of proton anisotropies was reported by Marsch et al. (1982) using Helios 1 and 2 data. In Fig. 15 from that paper, it can be seen that the Ulysses results are consistent with the Helios results as extrapolated to 1-4 AU. Inside 1 AU, they found that the anisotropy in the high speed solar wind was often less than unity, while it was as large as 2.0 in the low speed flow. These trends will be used below to show that using the values in Fig. 8, independent of radius, gives an upper bound to the amount of flux redistribution.

The analytic estimates in Eqs. (3) and (4) were made using an isotropic temperature and pressure. Because the temperature, and hence pressure anisotropy is larger than unity, the perpendicular pressure will be reduced relative to that shown in Fig. 3. Beyond this simple effect, the difference in pressure anisotropy between the high speed and the low speed solar wind means that the pressure gradient, or difference, between these two regimes will be further reduced. Hence, the effective meridional pressure variation is considerably smaller than shown by Fig. 3. Applying the anistoropies in Fig. 8 to the electron, proton, and alpha particle pressures used in Fig. 3 gives the result shown in Fig. 9.

This figure shows that the effective pressure for computing the meridional pressure gradient is far smaller than would be expected by considering only the isotropic pressure. Using again Eq. (7) to approximate the pressure, we now find that $\alpha = 3.33$, $\epsilon = 0.58$, and $p_E = 1.25 \times 10^{-10}$. The curve derived from these parameters is shown as the thin line in Fig. 9. Substituting these revised numbers into (11) gives $C = 0.49$ and

$$\frac{B_{2r}(r,\theta)}{B_{1r}(r)} \mid_{1AU} \approx 0.15 f_2(\theta) \qquad (13a)$$

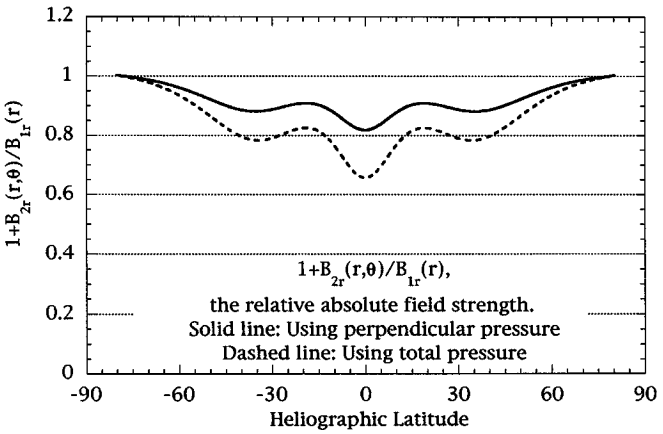

Fig. 10. The relative variatoin of the modeled magnetic field strength versus heliographic latitude at 1.0 AU for the perpendicular pressure shown in Fig. 9 (solid line). The relative variation using the isotropic pressure, also at 1 AU and taken from Fig. 6, is shown by the dahed line for comparison. $\epsilon = .58$, and $p_E = 1.25 \times 10^{-10}$ dynes/cm^2. The isotropic pressure from Fig. 3 is also shown for reference.

$$\frac{B_{2r}(r,\theta)}{B_{1r}(r)} \mid_{r\to\infty} \approx 0.21 f_2(\theta) \qquad (13b)$$

for the flux redistribution using the perpendicular pressure shown in Fig. 9. This is a much smaller effect than found in Eq. (12). A comparison of the calculated flux redistribution at 1 AU using the pressure shown in Fig. 3 with that found using the perpendicular pressure in Fig. 9 is shown in Fig. 10. The comparison is made at 1 AU and it is seen that the assumed anistropies shown in Fig. 8 result in about a 50% reduction in the computed flux redistribution.

Similarly, the maximum meridional flow speed is also reduced by about 50%, from 17 km/s to 9 km/s at 1 AU, at a latitude of 35^o.

The pressure anisotropy used here is independent of radius. If the radial variation observed by Marsch et al. (1982) had been invoked, the flux redistribution would have been reduced by approximately another 50%. This is because the difference in the perpendicular pressure between the high speed and low speed solar wind is smaller closer to the Sun than it is at 1-4 AU. This implies that the pressure anisotropy alone is enough to account for the discrepancy between the original calculation shown in Fig. 6 and the observations of IMP, ICE, and Ulysses.

4. Discussion

The conclusion from the analysis in Sect. 2 and Sect. 3 is that the meridional pressure distribution observed by Ulysses at 1.4-4 AU will not modify the distribution of magnetic flux already present in the solar wind at the top of the corona - 10 $R_\odot$. This conclusion would not have been possible if the pressure anisotropy were ignored.

With regard to the consistency of the analysis, reconsider the assumptions listed in Sect. 2. All of them seemed well-justified except (2) - that the radial flow speed be independent of radius. This approximation depends on how much solar wind acceleration occurs inside 10 $R_\odot$. Recent studies (e.g. Habbal et al. 1995) have suggested most of the solar wind wind acceleration is complete by this distance so the approximation is probably good. Classical solar wind models without added acceleration source terms have a much flatter speed profile in radius so that approximation (2) would be much less valid. However, in the end, the conclusion here that the meridional pressure gradient does not lead to a large magnetic flux redistribution means that the details of the flow speed profile in radius are not critical to the conclusion.

A critical assumption could have been ignoring stream interaction. This is not because of the driving of meridional flow due to pressure ridges associated with passing high speed streams. That process has been examined by Pizzo and Goldstein (1987) and found to be negligible. Instead, the heating by stream interaction can be an important source for the pressure bump. This means that near the Sun the pressure bump might have been smaller, and therefore the effective meridional transport reduced. However, the Ulysses fast latitude scan data was taken near solar minimum when the amount of heating by CIRs does not appear to be very large. Furthermore, coronal models imply that there will be a significant pressure bump in the signature of the streamers themselves (Suess et al. 1996). The dependence of $f_1(r)$ in (11) on radius can be used to investigate this, other limiting cases, and the consistency of the analysis. Taking the extreme case of a temperature being independent of radius gives $f_1(r) \propto \ln(r)$ and there is a secular increase of B_{2r} with radius. This case turns out to be analogous to redistribution due to internal MHD forces, where it was shown earlier (Suess and Nerney, 1973, 1975b) that the MHD effect is proportional to $\ln(r)$. In the MHD case meridional flow is driven by the gradient in B_ϕ^2 with latitude. Asymptotically, $B_\phi \propto (1/r)$ and the equivalent magnetic pressure is proportional to $(1/r)^2$. This is the same as the dependence of the thermal pressure on radius for an isothermal wind. Therefore, the two results are consistent with each other. The magnitude of the MHD effect is nevertheless very small in the inner solar system for the simple reason that $\beta > 1$ throughout the region under discussion. This places an upper bound, also, on what might be expected from a weaker radial dependence of temperature on radius, such as found by Richardson et al. (1995).

The pressure anisotropy is found to be the most important physical parameter for understanding the Ulysses observations of the distribution of B_r in latitude. The perpendicular pressure is smaller than the isotropic or parallel pressure, as suggested in Fig. 9. It is the perpendicular pressure that drives meridional transport and the anisotropy reduces the effective transport to about 50% of that predicted using an isotropic pressure. Considering that the pressure anisotropy shown in Fig. 9 is also a function of heliocentric distance and using the empirical results for this radial dependence given by Marsch et al. (1982) shows that meridional transport near solar minimum can be expected to be $\leq 10\%$ at 1 AU and $\leq 20\%$ at larger distances. It was shown earlier (Suess and Smith, 1996) that the field strength at 10 $R_\odot$

is constant except in the HPS so B_r should be independent of latitude on global scales between 10 $R_\odot$ and a few AU.

With regard to the quasi-radial flow approximation itself, recall that Eqs. (2), (3), and (4) have been linearized around radial flow and the meridional gradients of p_2 and B_{2r} have been ignored in computing $v_{2\theta}$. If these gradients become too large, they will resist continuing meridional flux redistribution. It can be, in other words, ultimately a self-limiting process if it continues rapidly in comparison to a solar wind expansion time. The amount of flux redistribution computed here during the Ulysses fast latitude scan is insufficient to lead to a significant back pressure at any location inside 10-20 AU so that this is not an important effect for the present study.

It is possible to reconstruct the analysis taking the back-pressure force into account, but this would have added unnecessary complexity to addressing the fundamental question of whether the problem might produce an interesting result in the first place. It is still possible that there will be significant meridional mass transport in the outer heliosphere due to the separate processes of heating due to corotating interaction regions and the meridional dependence of the IMF. However, that is not the topic of the present investigation.

Acknowledgements. The work has been partially supported by the NASA Ulysses Project (S.S.), the Jet Propulsion Laboratory, California Institute of Technology, under contract with NASA (E.S.), and by Los Alamos National Laboratory under the auspices of the U. S. Department of Energy with support from NASA (J.P.).

References

Balogh, A., E. J. Smith, B. T. Tsurutani, D. J. Southwood, R. J. Forsyth, and T. S. Horbury, 1995, Science, 268, 1007.

Burton, M. E., E. J. Smith, A. Balogh, and N. Murphy, 1996, proc. of Solar Wind 8 (D. Winterhalter, D. McComas, N. Murphy, and J. Phillips, eds.), in press.

Cole, J. D., 1968, Perturbation Methods in Applied Mathematics, Blaisdell, Waltham, Massachusetts.

Goldstein, B. E., M. Neugebauer, and E. J. Smith, 1995, Geophys. Res. Lett., 22, 3389.

Goldstein, B. E., M. Neugebauer, S. J. Bame, D. J. McComas, and J. L. Phillips, 1995, EOS, 76, 454.

Goldstein, B. E., E. J. Smith, J. T. Gosling, D. J. McComas, and A. Balogh, 1996, EOS, 77, 220.

Gosling, J. T., G. Borrini, J. R. Asbridge, S. J. Bame, W. C. Feldman, and R. T. Hansen, 1981, J. Geophys. Res., 86, 5438.

Habbal, S. R., R. Esser, M. Guhathakurta, and R. R. Fisher, 1995, Geophys. Res. Lett., 22, 1465.

Marsch, E., K.-H. Mülhäuser, R. Schwenn, H. Rosenbauer, W. Pilipp, and F. M. Neubauer, 1982, J. Geophs. Res., 87, 52.

Munro, R. H., and B. V. Jackson, 1977, Astrophys. J., 213, 874.

Phillips, J. L., S. J. Bame, A. Barnes, B. L. Barraclough, W. C. Feldman, B. E. Goldstein, J. T. Gosling, G. W. Hoogeveen, D. J. McComas, M. Neugebauer, and S. T. Suess, 1995, Geophys. Res. Lett., 22, 3301.

Pizzo, V. J., and B. E. Goldstein, 1987, J. Geophys. Res., 92, 7241.

Richardson, J. D., K. I. Paularena, A. J. Lazarus, and J. W. Belcher, 1995, Geophys. Res. Lett., 22, 325.

Smith, E. J., and A. Balogh, 1995, Geophys. Res. Lett., 22, 3317.

Suess, S. T., and S. F. Nerney, 1973, Astrophys. J., 184, 17.

Suess, S. T., and S. F. Nerney, 1975a, Solar Phys., 40, 487.

Suess, S. T., and S. F. Nerney, 1975b, Geophys. Res. Lett., 2, 75.

Suess, S. T., A. K. Richter, C. R. Winge, and S. F. Nerney, 1977, Astrophys. J., 217, 296.

Suess, S. T., and E. J. Smith, 1996, Geophys. Res. Lett., submitted.

Suess, S. T., A.-H. Wang, and S. T. Wu, 1996, J. Geophys. Res., in press.

Wolfson, R., 1985, Astrophys. J., 288, 769.